Effect of source temperature on phase and metal–insulator transition temperature of vanadium oxide films grown by atomic layer deposition*

Bingheng Meng(孟兵恒), Dengkui Wang(王登魁)†, Deshuang Guo(郭德双), Juncheng Liu(刘俊成), Xuan Fang(方铉), Jilong Tang(唐吉龙), Fengyuan Lin(林逢源), Xinwei Wang(王新伟), Dan Fang(房丹), and Zhipeng Wei(魏志鹏)‡

State Key Laboratory of High Power Semiconductor Laser, Changchun University of Science and Technology, Changchun 130022, *China*

(Received 16 January 2020; revised manuscript received 30 July 2020; accepted manuscript online 13 August 2020)

Vanadium oxide films were grown by atomic layer deposition using the tetrakis[ethylmethylamino] vanadium as the vanadium precursor and H_2O as the oxide source. The effect of the source temperature on the quality of vanadium oxide films and valence state was investigated. The crystallinity, surface morphology, film thickness, and photoelectric properties of the films were characterized by x-ray diffraction, atomic force microscope, scanning electron microscope, *I–V* characteristics curves, and UV–visible spectrophotometer. By varying the source temperature, the content of V_6O_{11}, VO_2, and V_6O_{13} in the vanadium oxide film increased, that is, as the temperature increased, the average oxidation state generally decreased to a lower value, which is attributed to the rising of the vapor pressure and the change of the ionization degree for organometallics. Meanwhile, the root-mean-square roughness decreased and the metal–insulator transition temperature reduced. Our study is great significance for the fabrication of vanadium oxide films by atomic layer deposition.

Keywords: vanadium oxide films, atomic layer deposition, source temperature, valence state

PACS: 71.30.+h, 61.50.Nw, 61.05.cp **DOI:** 10.1088/1674-1056/abaee7

1. Introduction

Vanadium oxide (VO_x) has attracted much interest due to its polymorphism and wide applications in a variety of fields.[1] Among the vanadium oxides, VO_2 has attracted significant attention due to its remarkable metal–insulator transition (MIT). This property makes it interesting for smart windows,[2–4] resistive memories, switches in microelectronics,[5–7] and batteries.[8] In addition, V_2O_5, V_6O_{11}, and V_6O_{13} also exhibit MIT, but their MIT temperatures are very different.[9–11] In fact, the V–O system has been reported to contain about 25 compounds.[12] It is experimentally challenging to control the optimum combination that would result in the accurate mixture of vanadium and oxygen in the desired proportion.

Thin films of stoichiometric vanadium oxide are not easily prepared considering that vanadium exists in many stable oxidation states and as an oxide in several polymorphic forms. VO_x films have been deposited using various techniques, such as pulsed laser deposition,[13] chemical vapour deposition,[14] sol-gel,[15] reactive sputtering,[16] electron beam evaporation,[17] and atomic layer deposition (ALD).[18] The key feature for ALD is the self-limiting character of the surface reactions, making layer by layer growth possible. Compared to other deposition techniques, its main advantages include the excellent control of thickness and stoichiometry. In recent years, some researchers have studied the effects of growth conditions, such as deposition temperatures, annealing temperature, and precursors on the crystalline of VO_x films.[16,18] However, the ionization degree of organometallics is varied with the source temperatures, which also greatly affects the structure of vanadium oxide. It needs further investigation.

Since the contents of ions in tetrakis[ethylmethylamino] vanadium (TEMAV) are different at different temperatures, which affects the valence state of vanadium oxide in the film. And VO_x is a complex system where subtle changes in deposition can lead to different phases being formed. Therefore, in this work, three vanadium oxide film samples were grown at the source temperature from 90 ℃ to 110 ℃. It was found that with source temperature increasing, the *x* value of VO_x film reduced and the MIT temperature of VO_x decreased.

2. Material and methods

VO_x films were grown on sapphire substrates using LabNanoTM 9000 Thermal ALD system. TEMAV and H_2O were employed as vanadium precursor and oxide source, respectively. N_2 was used as the carrier gas. The growth program designed for this study consisted of the pulse sequence of 0.02 s/12 s/0.04 s/32 s for vapor pulse/purge/TEMAV

*Project supported by the National Natural Science Foundation of China (Grant Nos. 11674038, 61674021, 61704011, and 61904017), the Developing Project of Science and Technology of Jilin Province, China (Grant Nos. 20170520118JH and 20160520027JH), and the Youth Foundation of Changchun University of Science and Technology (Grant No. XQNJJ-2018-18).

†Corresponding author. E-mail: wccwss@foxmail.com

‡Corresponding author. E-mail: zpweicust@126.com

© 2020 Chinese Physical Society and IOP Publishing Ltd

pulse/purge, which was executed 1500 cycles. During the deposition process, the substrate temperature was kept at 200 ℃. The source temperatures of TEMAV were kept at 90 ℃, 100 ℃, and 110 ℃ for different samples, which are labeled A, B, and C, respectively.

The surface morphology and thickness of the film were characterized by atomic force microscope (AFM) and scanning electron microscope (SEM), respectively. The crystallinity was studied by x-ray diffraction (XRD, Bruker D8 Focus). The absorption spectrum was measured by UV–visible spectrophotometer (UV-2450) and the performances of MIT of VO_x films were analyzed using a source meter unit (Keithley 2400).

3. Results and discussion

In order to study the relationship between the source temperature and surface morphology of VO_x, the samples were tested by AFM. AFM measurement revealed the tendency of surface structure more clearly. Figures 1(a)–1(c) show the AFM images for VO_x deposited under various conditions. The detailed profiles of surface, within a 2 μm×2 μm image window, are observed in those figures. Roughness was calculated as root-mean-square values (RMS). The RMS of samples A, B, and C are approximately 1.27 nm, 1.13 nm, and 0.45 nm, respectively, which is consistent with reports.[14] As the temperature of the vanadium source increases, the vapor pressure of TEMAV increases. However, the pulse time and purge time have not been adjusted accordingly, which leads to the increase of precursor concentration on the grown surface.[19] Hence, with source temperature increasing, the growth rate of the vanadium oxide increases and the surface morphology becomes flat. Furthermore, in order to study the relationship between the source temperature and thickness of VO_x, the samples were tested by SEM. As can be seen from Figs. 1(d)–1(f), the thicknesses are 3.9 μm, 4.0 μm, and 4.2 μm for samples A, B, and C, respectively. The thicknesses of films deposition at different source temperatures are almost the same.

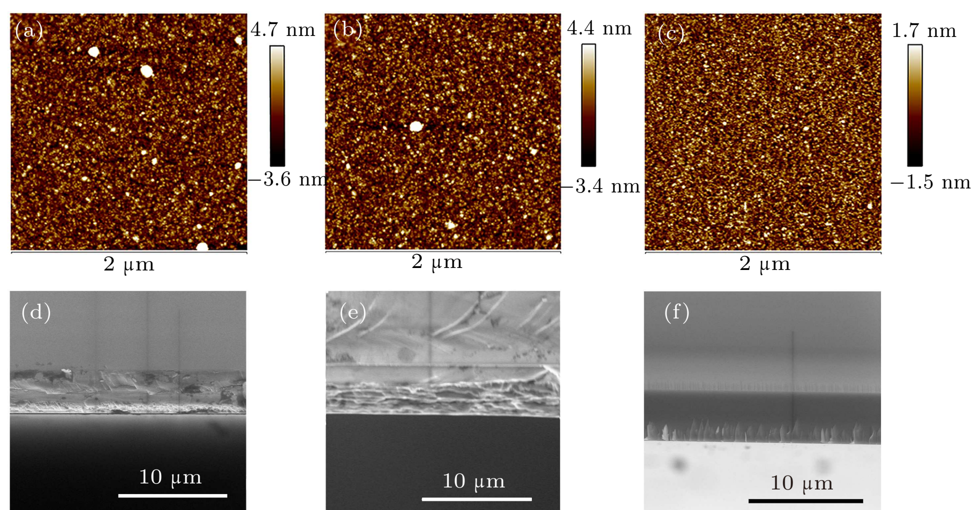

Fig. 1. (a)–(c) The AFM images of samples A–C. (d)–(f) The SEM micrographs in cross-sectional view of samples A–C.

The properties of vanadium oxide films largely depend on the stoichiometry, structure, and morphology.[20] In order to study the effect of the precursor temperatures on the structure of VO_x, the samples were characterized by using XRD, as shown in Fig. 2. The XRD spectra show that the phases of VO_x are very different for the three samples. At the source temperature of 90 ℃, the main phase of vanadium oxide is V_2O_5. However, when the source temperature is 100 ℃ or 110 ℃, an amount of V_6O_{11} and V_6O_{13} phases appear in the film, and the V_4O_9 phase disappears. It indicates that the valence states of vanadium transit from high valence states to low valence states with the increase of the source temperature. As reported by Monnier,[21] $V(NEtMe)_4^+$, $V(NEtMe)_3^+$, $V(NEtMe)_2^+$, $VNEtMe^+$, and $NEtMe^+$ ions formed from TEMAV ionization. $V(NEtMe)_4^+$ is the parent ion of TEMAZ, while $V(NEtMe)_3^+$, $V(NEtMe)_2^+$, $VNEtMe^+$, and $NEtMe^+$ are fragment ions. And the ionization potentials of $V(NEtMe)_4^+$, $NEtMe^+$, $V(NEtMe)_3^+$, $V(NEtMe)_2^+$, and $VNEtMe^+$ increase in turn. The influence of the temperature is more complex since the phases have no time to settle to an equilibrium state at each temperature, so thin-film kinetics will complicate this behavior.[22] The relative strength of the diffraction peak in XRD spectra is proportional to the composition of the corresponding material in the film. So, the relative strength can be used to compare the changes of the proportion of the corresponding components in different films.[23,24] When the source temperature is 90 ℃, the mixing phase in the film is dominated by the V_2O_5 relative peak strength. With the source temperature increasing, the relative peak strength of V_6O_{11} and V_6O_{13} increases and the relative peak strength of

V_2O_5 decreases. However, the average oxidation state generally decreases to a lower value as the temperature increases, indicating the higher temperature stability of the lower oxides, as shown in Table 1. The experimental results of van Heerden[23] and Criado[24] also showed that the corresponding peak strength increases with the increase of the concentration of the substance, and the other deposition conditions remain unchanged.

The absorption spectrum was used to measure the optical band gap. Figure 3 (a) shows the absorption spectra of the three VO_x films. With the source temperature increasing from 90 ℃ to 110 ℃, the absorption edge red-shifts from 355 nm to 450 nm. The optical band gap can be estimated by the formula $(\alpha h\nu)^2 = A^2(h\nu - E_g)$,[25] where A^2, α, h, ν, and E_g are the direct transition constant, the optical absorption coefficient, the Planck constant, the photon frequency, and the optical band gap, respectively. For direct transition, the optical band gap E_g can be obtained from the intercept of $(\alpha h\nu)^2$ to $h\nu$. The optical band gaps of different samples are calculated by extrapolation, as shown in the illustrations. Their optical band gaps are 3.50 eV, 3.08 eV, and 2.74 eV, respectively. Namely, with the source temperature increasing, the band gap decreases and the absorption edge red-shifts.

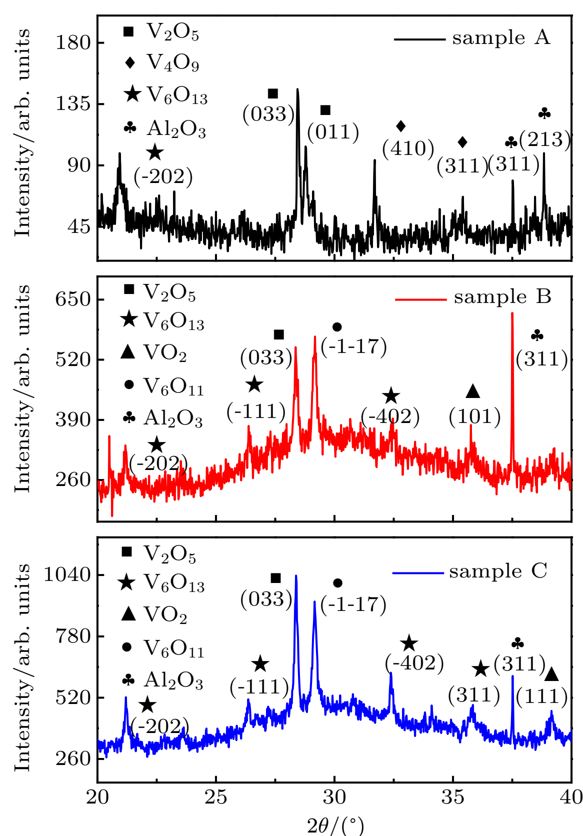

Fig. 2. The XRD pattern of VO_x films deposited on sapphire substrate with different source temperatures: (a) 90 ℃, (b) 100 ℃, and (c) 110 ℃.

Table 1. Variation of the ratio of the strongest integrated intensity of each vanadium oxide in the film to the strongest integrated intensity of the substrate peak with the source temperature.

Source temperature/℃	$I_{V_2O_5}/I_{Al_2O_3}$	$I_{V_4O_9}/I_{Al_2O_3}$	$I_{V_6O_{13}}/I_{Al_2O_3}$	$I_{VO_2}/I_{Al_2O_3}$	$I_{V_6O_{11}}/I_{Al_2O_3}$
90	3.09	2.24	1.91	0	0
100	3.51	0	1.08	1.37	3.57
110	7.27	0	2.31	3.86	10.12

The band gap is determined by the top of the valence band and the bottom of the conduction band. The change of the band gap is due to the change of the electronic structure of the crystal, so we analyzed the thin films at different temperatures. According to the XRD pattern, as the source temperature increases, the x value of VO_x decreases, that is, the contents of V_6O_{11} and V_6O_{13} increase significantly. As reported in the literature,[9,10] the metal–insulator transitions of V_6O_{11} and V_6O_{13} at −103 ℃ and −128 ℃ are accompanied by a structural transformation. The V_6O_{11} and V_6O_{13} exhibit the metallicity at room temperature, which makes the metal state valence band hybrid. According to the Goodenough band theory,[26] the phase transition temperature of vanadium oxide films mainly depends on the energy level structure. In the UV–Vis absorb spectra, with the increase of the source temperature, the absorption edges of the corresponding films show a red shift, indicating that the band gap is narrowed due to the valence band hybridization. Therefore, the carrier concentration in the film increases, which results in the decrease of the band gap of the film. The optical transmission spectra of the as-deposited VO_x thin films on sapphire substrates at various deposition temperatures are shown in Fig. 3(b). It can be seen from the transmission diagram that the transmittance of the film increases with the decrease of the source temperature. This is due to the increased content of V_6O_{11} or V_6O_{13} in the film mixed phase during the process of increasing the source temperature. However, the V_6O_{11} or V_6O_{13} exhibits metallic properties at room temperature, so the free electron conduction in the film increases sharply and the optical properties change obviously. The absorption of free electron to light will lead to the decrease of optical transmittance. Both of these results indicate that the content of low-valence vanadium oxide in the film mixture increases after the source temperature increases.

The I–V curves of all samples were measured at various temperatures and the conductivity was calculated from Ohm's law. The relations of conductivity and temperature are presented in Fig. 4. The conductivity of the samples increases with temperature rising. It is worth noting that the conductivity of samples B and C is significantly higher than that of sample A and the conductivity of sample C has an abrupt rise at about 208 ℃, which means the metal–insulator transition occurs. According to the previous analyze, when the temperature

of the vanadium source increases, the content of V_6O_{11} and V_6O_{13} phase increases obviously. The metal–insulator transitions of V_6O_{11} and V_6O_{13} occur at −103 ℃ and −128 ℃, respectively, which are lower than that of the main phase (VO_2: 68 ℃ and V_2O_5 258 ℃) in the film.[9–11] The phase transition temperature of vanadium oxide films mainly depends on the energy level structure. The narrower the band gap, the lower the phase transition temperature. In films prepared at temperatures of 90 ℃ and 100 ℃, V_2O_5 dominates. And the V_2O_5 phase transition temperature is 258 ℃, so there is no phase transition process in the test range. The absorption curve also shows that the band gap of the films decreases gradually after the source temperature increases. So, the increase of V_6O_{11} and V_6O_{13} phase content in samples B and C results in the increase of the conductivity and the decrease of the metal–insulator transition temperature. These results are consistent with the XRD pattern.

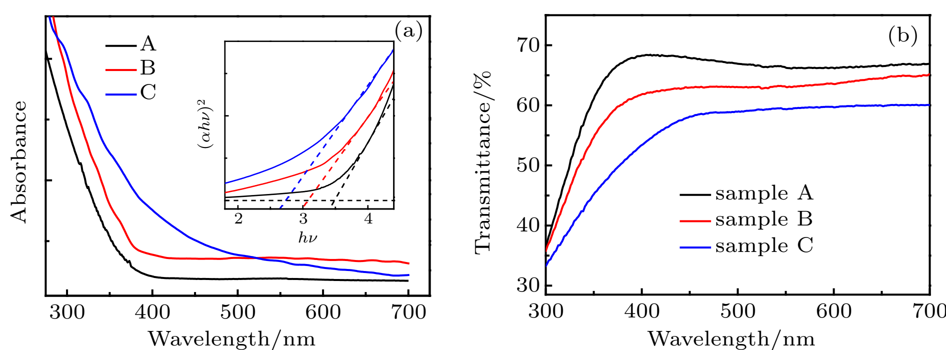

Fig. 3. (a) The absorption spectra and (b) transmission spectra of samples A–C.

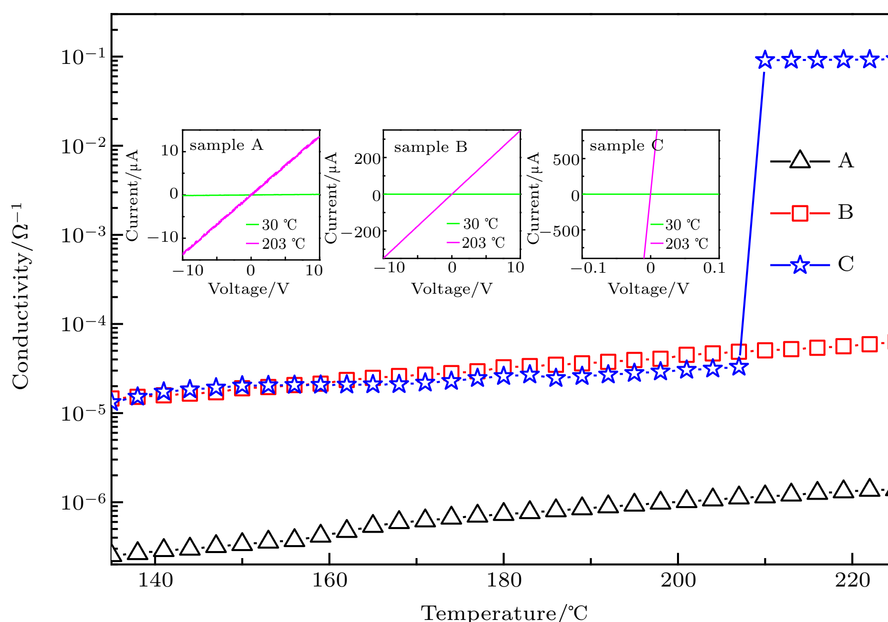

Fig. 4. The relation of conductivity and temperature. The insets show the *I–V* curves at 30 ℃ and 208 ℃ for samples A–C.

4. Conclusions

In summary, our work presents a detailed report on the growth of atomic layer deposited vanadium oxide thin films at different source temperatures. Vanadium oxide films could be grown by using water as the oxygen source and TEMAV as the vanadium precursor. The formation mechanism of these phases was discussed. The relationship between surface morphology of VO_x and source temperature was studied. With the increase of the source temperature, the surface morphology of the film is improved, the absorption edge appears red shift, the conductivity increases, and the metal–insulator transition temperature decreases. These phenomena were attributed to the rising of vapor pressure and the change of ionization degree for organometallics, which caused by the increase of the source temperature. Our results are of important significance to manage the structure and properties of vanadium oxides films.

References

[1] Yang Z, Ko C and Ramanathan S 2011 *Annu. Rev. Mater. Res.* **41** 337

[2] Cui Y Y, Ke Y J, Liu C, Chen Z, Wang N, Zhang L M, Zhou Y, Wang S C, Ga Y F and Long Y 2018 *Joule* **2** 1

[3] Shao Z W, Cao X, Zhang Q X, Long S W, Chang T C, Xu F, Yang Y and Jin P 2019 *Sol. Energ. Mater. Sol. C* **200** 110044

[4] Xu F, Cao X, Luo H and Jin P 2018 *J. Mater. Chem. C* **6** 1903

[5] Son M, Lee J, Park J, Shin J, Choi G, Jung S, Lee W, Kim S, Park S and Hwang H 2011 *IEEE Electr. Device L.* **32** 1579

[6] Wang Z L, Zhang Z H, Zhao Z, Shao R W and Sui M L 2018 *Acta Phys. Sin.* **67** 177201 (in Chinese)

[7] Sun X N, Qu Z M, Wang Q G, Yuan Y and Liu S H 2019 *Acta Phys. Sin.* **68** 107201 (in Chinese)

[8] Chen X Y, Pomerantseva E, Banerjee P, Gregorczyk K, Ghodssi R and Rubloff G 2012 *Chem. Mater.* **24** 1255

[9] Schwingenschlögl U, Eyert V and Eckern U 2003 *Euro Phy. Lett.* **61** 361

[10] Shin S, Suga S, Taniguchi M, Fujisawa M, Kanzaki H, Fujimori A, Daimon H, Ueda Y, Kosuge K and Kachi S 1990 *Phys. Rev. B* **41** 4993

[11] Raja S, Subramani G, Bheeman D, Rajamani R and Bellan C 2016 *Optik* **127** 461

[12] Wriedt H A 1989 *Bull. Alloy Phase Diagrams* **10** 271

[13] Chiu T W, Tonooka K and Kikuchi N 2010 *Thin Solid Films* **518** 7441

[14] Nandakumar N K and Seebauer E G 2011 *Thin Solid Films* **519** 3663

[15] Hanlon T J, Walker R E, Coath J A and Richardson M A 2002 *Thin Solid Films* **405** 234

[16] Yun S J, Lim J W, Noh J S, Chae B G and Kim H T 2008 *Jpn. J. Appl. Phys.* **47** 3067

[17] Subrahmanyam A, Reddy Y B K and Nagendra C L 2008 *J. Phys. D: Appl. Phys.* **41** 195108

[18] Blanquart T, Niinistö J, Gavagnin M, Longo V, Heikkilä M, Puukilainen E, Pallem V R, Dussarrat C, Ritala M and Leskelä M 2013 *RSC Adv.* **3** 1179

[19] Rampelberg G, Deduytsche D, Schutter B D, Premkumar P A, Toeller M, Schaekers M, Martens K, Radu I and Detavernier C 2014 *Thin Solid Films* **550** 59

[20] Griffiths C H and Eastwood H K 1974 *J. Appl. Phys.* **45** 2201

[21] Monnier D, Nuta I, Chatillon C, Gros-Jean M, Volpi F and Blanquet E 2009 *J. Electrochem. Soc.* **156** H71

[22] Mattelaer F, Geryl K, Rampelberg G, Dobbelaere T, Dendooven J and Detavernier C 2016 *RSC Adv.* **6** 114658

[23] Van Heerden J L and Swanepoel R 1997 *Thin Solid Films* **299** 72

[24] Criado M, Fernández-Jiménez A, de la Torre A G, Aranda M A G and Palomo A 2007 *Cem. Concr. Res.* **37** 671

[25] Li W, Wang D K, Zhang Z Z, Chu X Y, Fang X, Wang X W, Fang D, Lin F Y, Wang X H and Wei Z P 2018 *Opt. Mater. Express* **8** 3561

[26] Goodenough J B 1971 *J. Solid State Chem.* **3** 490